Exploring soliton enhancement for ground-based detection of lethal non-trackable space debris

Kristine Rosfjord, Kristen Shavlik, Jeremy Kolansky, W.J. Mandeville
InTrack Radar Technologies
Piyush Mehta
West Virginia University

ABSTRACT

The detection of small lethal non-trackable (LNT) objects is beyond the capabilities of existing detection systems, yet the need for the detection of these objects increases with their growing prevalence. Here we investigate the existing critical challenges of implementing a ground-based end-to-end soliton detection system for the identification and tracking of LNTs and highlight three challenges to the realization of this system. These include (1) the propagation of a high frequency (HF) radar signal requires frequencies above 10 MHz; (2) limiting the spectral range to above 10 MHz negates the ability of the soliton to reflect the incident wave for a set of realistic space soliton parameters; (3) the path distortion through the ionosphere suggests a bistatic/multistatic system is required to receive a signal. Future work will include an exploration of both hybrid ground/space and space-based detection systems.

1. MOTIVATION

There is a growing desire to be able to detect and track centimeter sized and smaller debris in low earth orbit (LEO). Current statistical analysis estimates that there are 100 million lethal non-trackable (LNT) objects in LEO that could cause significant damage to operational satellites and crewed missions. Traditional space surveillance sensors are limited to detecting and tracking debris that is several centimeters in diameter or larger. Surveying large areas and detecting smaller objects is challenging due to their small optical and/or radar cross section. Recent laboratory investigations [12] have explored nonlinear plasma waves generated by small, charged objects in a flowing ion field. These nonlinear waves are known as electromagnetic solitons. These solitons can be pinned or precursor depending on whether they are stationary relative to the object or emanating in front of the object. Solitons generated by LNT objects traveling through the ionosphere may offer an opportunity to leverage a detection scheme that could offer a significantly larger observable cross section than the debris hard-body itself. It is an open challenge, however, whether the community will be able to detect and track these pinned and/or precursor solitons from the ground. As a part of the IARPA SINTRA program, we are pursuing methods for the ground-based identification of precursor and/or pinned solitons generated by small debris in LEO.

Previous research and development in ground-based space surveillance has enabled detection and tracking of debris several centimeters in size and larger, but it has fallen short of reliably identifying LNT objects in LEO. Wide field-of-view (WFOV) systems, while covering large areas of the sky, lack the sensitivity needed to detect smaller objects. Narrow field-of-view (NFOV) systems, though more sensitive, often require a priori knowledge of debris motion and are constrained by their limited coverage. This trade-off has led systems like the U.S. Space Surveillance Network (SSN) to be effective for tracking debris larger than 10 cm. However, with an increasing need to detect smaller, but still dangerous debris, traditional methods are insufficient. This gap is why we are exploring innovative approaches, such as leveraging solitons generated by small debris moving through the ionosphere, to address this critical challenge [11].

Recent research has begun to explore innovative approaches for detecting small debris through the observation of electromagnetic solitons generated by charged objects moving through the ionosphere. For example, DesJardin and Hartzell investigated how plasma interactions, specifically solitons, can be leveraged for detecting sub-centimeter space debris, suggesting that these interactions could provide a larger observable cross-section than the debris itself [4,

5]. Additionally, Truitt and Hartzell characterized plasma solitons produced by small orbital debris, further supporting the potential of solitons in enhancing detection capabilities for smaller objects [14, 15]. Other researchers, such as Bernhardt et al., have also observed plasma waves generated by space objects, emphasizing the growing interest in using nonlinear plasma phenomena for space debris detection [2]. These studies collectively pave the way for follow on work to investigate potential system solutions to detecting and tracking LNTs.

2. APPROACH

Here we evaluate the potential of a ground-based system for the LEO detection of small debris utilizing plasma solitons. In contrast with hard-body detection of LNTs, precursor solitons generated by these debris may offer an alternative detection modality to hard-body detection. Precursor solitons also provide a quasi-periodic structure that may offer resonant scattering that could help enhance remote detection. In tandem with these advantages, there are challenges associated with creating a ground-based, end-to-end soliton detection system. Referring to Fig. 1, a ground-based system first needs to successfully propagate through the ionosphere and not be reflected/refracted back to earth before reaching the LNT. Second, when reaching the LNT, the frequency of the propagated wave must be able to interact with the higher-density soliton so that it can be returned to ground. Third, upon successful return to ground, the location of that return must be a known quantity. These three challenges are labeled in Fig. 1 as A, B, and C respectively.

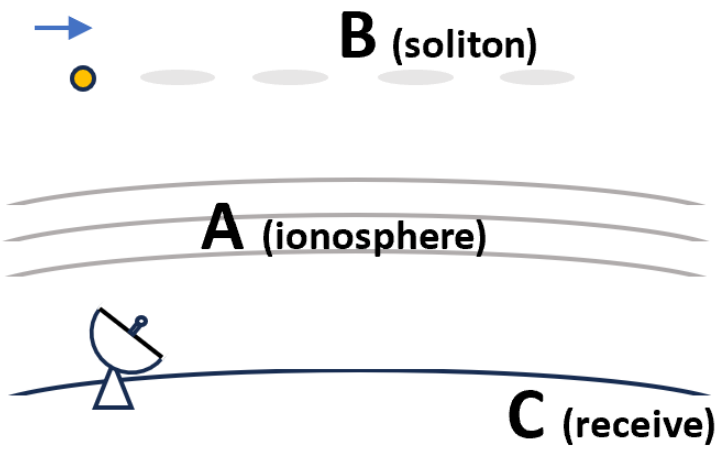

Fig. 1: System view of a ground-based end-to-end soliton detection.

In this paper we investigate the three key challenges labeled in Fig. 1 for ground-based precursor soliton detection and explore some possible mitigation paths. One of the goals of this research is to measure the plasma density change associated with an LNT's soliton wave. As we will see, this plasma density difference between the higher-density and background density portions of a train of precursor solitons plays an important role in understanding radar signal interaction with the train. Ionosonde radars, which operate in the high frequency (HF) range, are often used to measure the plasma density in the ionosphere. Based on this knowledge, our study is performed utilizing the HF interrogation range of 1–30 MHz. HF electromagnetic waves that pass into the ionosphere are refracted in various ways according to the frequency of the wave and the electron density in the ionosphere where the wave passes. Additional effects from the Earth's magnetic field and collisions from ions in the D layer affect the trajectory of the waves, though much less so than the electron density. To understand how these effects impact signal traveling from the ground through the ionosphere (as shown in A of Fig. 1), we implement HF propagation through numerical ray tracing, based on the algorithms specified in [6] and [9].

Once a signal makes it through the atmosphere, we explore the interaction of an HF signal with either a single pinned soliton or a train of precursor solitons, which we consider as a distributed Bragg reflector or a multilayer stack (B in Fig. 1). Soliton parameters, including soliton full width half max and the distance between solitons for a given debris radius, altitude, and temperature, are determined using MATLAB [7, 8] code [1] based off the forced Korteweg-de

Vries (fKdV) equations as presented in [14] and [15]. These parameters are used to determine reflection based upon the soliton structure using the commercial finite element method software COMSOL Multiphysics® [3]. Finally, we analyze how the signal might return to the ground as depicted in Fig. 1 using our ray tracer. Combined, the methods presented in this study lay the groundwork needed to conduct further studies of additional detection schemes.

3. RADIATION PROPAGATION TO SOLITON

As shown in Fig. 1, a ground-based system must first be able to propagate through the atmosphere to the soliton under test. For HF radiation, if the plasma frequency of the background is equal to the frequency of the propagating wave, this wave will be refracted back towards the ground [9, 13]. The plasma frequency is defined as

$$f_p = \frac{1}{2\pi}\sqrt{\frac{N_e e_2}{\varepsilon_0 m_e}}, \tag{1}$$

where N_e is the number of electrons in the area, e is the elementary charge, ε_0 is the vacuum permittivity, and m_e is the mass of an electron at rest [10]. Another way to look at this is that the propagating wave is reflected to earth when the critical factor X is approximately equal to 1. This critical factor is defined as

$$X = \frac{f_p^2}{f_{wave}^2}.$$

The numerical HF ray tracing technique employed here [6, 9] is validated using the IRI 2016 model. Fig. 2 shows the calculated wave height for a given plasma frequency from the IRI model (blue line) and the HR ray tracing technique (green dots).

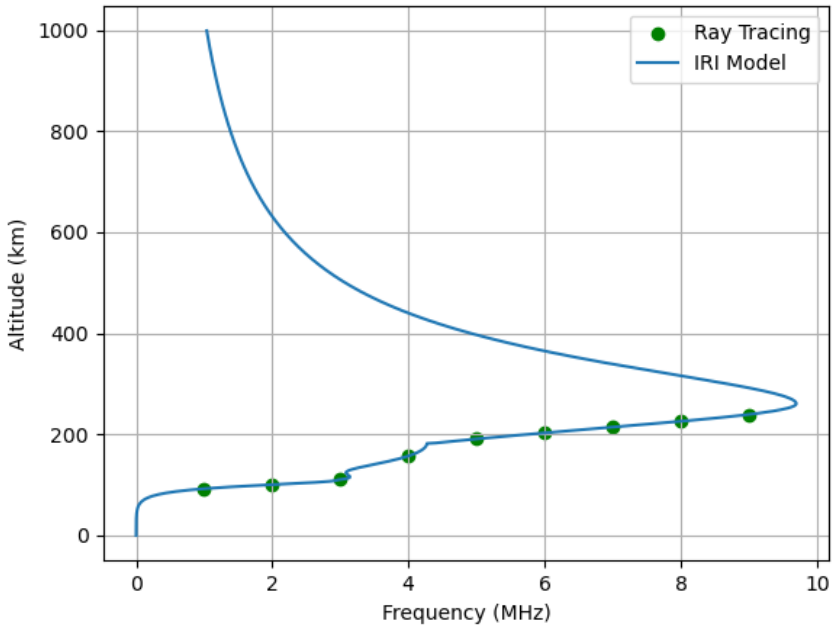

Fig. 2: The blue line is taken from the IRI model and shows the plasma frequency as a function of altitude. The green dots are calculated using the ray tracing technique showing the maximum propagation height (at zenith).

Using the validated HF ray tracing technique, this critical factor is plotted in Fig. 3 versus altitude above the earth's surface for four discrete frequencies in the HF regime for a wave launched directly up towards the ionosphere. As seen in Fig. 3, the lowest frequency (1 MHz) reaches a critical factor of 1 at approximately 93 km. This means that 1 MHz radiation is stopped by the ionosphere's E-layer and reflected to ground. The 7 MHz radiation reaches a critical factor of 1 at approximately 219 km and is reflected to the ground by the F-layer of the ionosphere. It's important to

note here that these reflections occur even without a soliton being present. Generally, frequencies greater than 10 MHz propagate through the F-layer, as illustrated in Fig. 2, and escape to space, but this depends on the plasma density, which can change quite significantly from day to day.

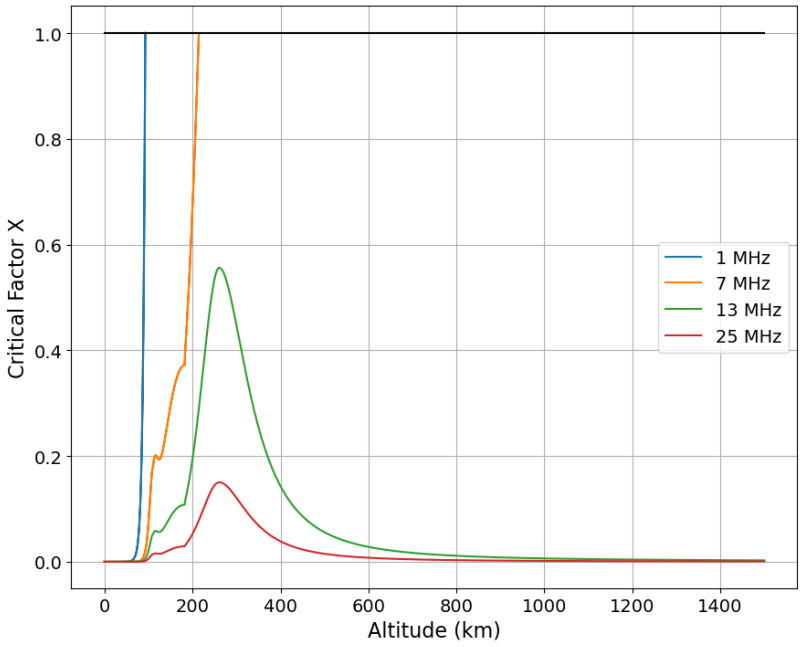

Fig. 3: Altitude versus the critical factor X for a selection of frequencies in the HF range.

Based on previous research and fKdV investigations done as part of our research, it is unlikely that solitons will be produced by debris at lower altitudes [14, 15]. As such, the ray tracing results suggest only frequencies above 10 MHz can reach our LNT of interest and its corresponding soliton.

It is critical to note that these lower frequencies do not propagate to where we might expect to find solitons generated by LNTs [14, 15]. In the approach presented above, the wave will only reflect an appreciable amount once X is approximately 1, i.e. the square of the plasma frequency is equal to the square of the wave frequency. From the relationship in equation (1), we observe that the square of the plasma frequency is linearly dependent on the plasma density and thus will change with a soliton density change. In the 1–10 MHz region, a 30% plasma density change implies a plasma frequency change of 30% also. Discussion of the upper frequency bound based upon the frequency dependence of the index of refraction is presented in the next section.

This analysis is performed with the assumption that the waves are launched vertically upward. For waves launched with angles less than vertical, the criteria for a reflection are significantly more complicated. These criteria will be discussed more depth in Section 5.

4. SOLITON REFLECTION

After successfully propagating to the soliton of interest, the next challenge, as shown in Fig. 1, is the ability to reflect off the soliton train. In the previous section, a critical factor less than one is required for propagation through the atmosphere. If we consider a single pinned soliton, the critical factor associated with the plasma density of the soliton must equal one to allow for reflection from that soliton. Fig. 4 demonstrates the plasma density increase of the soliton peak over the background that is necessary to create a critical factor equal to 1 and thus a reflection to ground. Note that at 1400 km altitude, plasma density enhancements of $30,400\%$ and $120,000\%$ are required for reflection at 13 MHz and 25 MHz, respectively. These density enhancement values are not of the same order of magnitude of the approximately 300% density enhancement at 1400 km calculated from the fKdV equations.

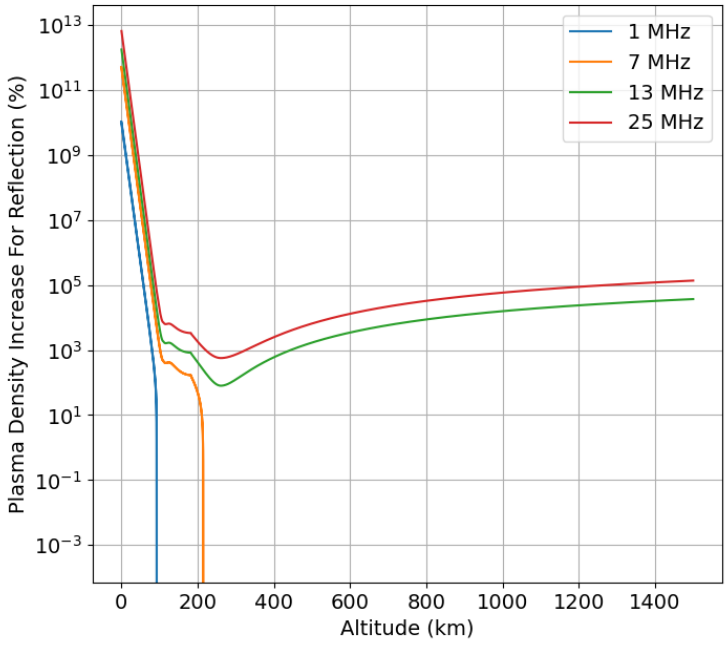

Fig. 4: Plasma density increase necessary for a ray of given frequency to propagate to a certain altitude.

Our modeling of the return from the soliton above is coarse and does not consider the specific geometry of the soliton. Here we move away from the approach of a bulk return that may be appropriate for a pinned soliton and use the periodic nature of precursor solitons to look at possible HF interactions within the Fraunhofer region. Our soliton input parameters, as calculated from fKdV simulation code [14, 15], for a debris radius of 2 cm at 1400 km in altitude are 0.8 m for the distance between solitons peaks and 0.13 m for the soliton width. We will represent a soliton train by a 31-layer multi-layer stack, with the 0.13 m layers representing the higher density soliton peaks and the 0.67 m layers representing the lower, background density regions in between solitons.

Because we have two distinct density regions, each will have its own index of refraction, which are plasma density and radar frequency dependent. To verify our multi-layer stack set up, we choose two indices of refraction that are far enough apart to demonstrate we can obtain expected results: 0.9 for the higher density regions and 1.25 for the lower density regions. We yield the results shown in Fig. 5 when sweeping the frequency from 1–500 MHz.

In Fig. 5 we note peaks in reflectance centered at roughly 160, 320, and 470 MHz. This indicates that if signal frequencies near the reflectance peaks were to generate refraction indices of 0.9 and 1.25, we could expect an incident wave to reflect off the soliton train. This figure is similar to the sorts of plots typically seen for multi-layer reflectors but is still not using the full set of space-based soliton and plasma parameters.

For a more realistic space environment, we utilized an electron temperature generated by the IRI 2020 model of 4061.58 K and a plasma frequency taken from our ray tracer of 0.7226 MHz. The index of refraction for the lower density regions is calculated using our ray tracer. The index for the higher density regions is calculated according to a simplified version of the Appleton-Hartree index of refraction equation

$$n_H = \sqrt{1 - m \cdot n_L^2},$$

where n_H is the index for the higher-density soliton, m is one plus the density increase (represented in decimal form) for a soliton peak over the background, and n_L is the index for the lower-density background plasma. Based on fKdV simulation results, we estimate a 300% change in soliton density. Since lower frequencies produce a larger difference in the two indices of refraction, we choose 3 MHz to be our frequency of study and calculate indices accordingly. For reflection off the soliton train to occur, we would need to see a peak in the reflectance plot near 3 MHz. The resulting plot is shown in Fig. 6.

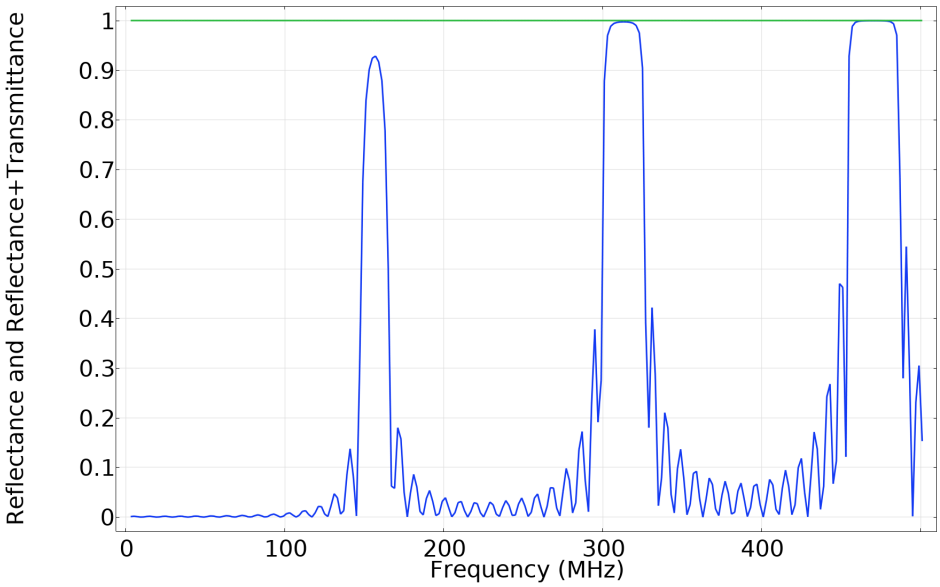

Fig. 5: Frequency versus reflectance for a 31-layer stack with higher density regions of 0.13 m with an index of refraction of 0.9 and lower density regions of 0.67 m with an index of 1.25. The green line is the total reflectance plus transmittance and the blue line is the reflectance alone.

As can be seen from the figure, there is no significant peak in reflectance near 3 MHz, so a 3 MHz wave is highly unlikely to reflect off a soliton train. Higher frequencies will produce indices that are closer together. As indices become closer, reflectance peaks narrow and decrease in height. This can be observed in Fig. 7, where the very minimal reflectance decreases asymptotically as frequency increases.

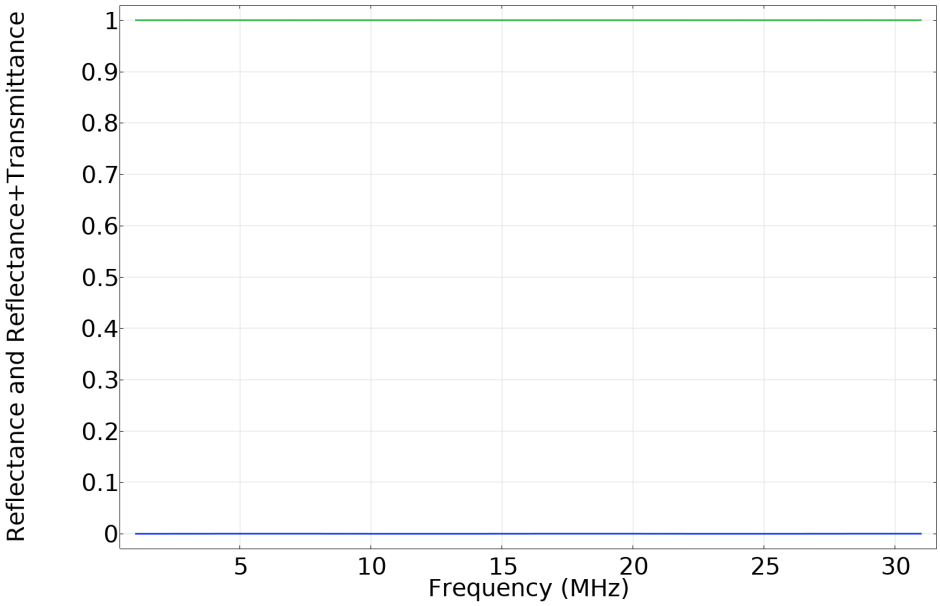

Fig. 6: Frequency versus reflectance for a 31-layer stack with higher density regions of 0.13 m with an index of refraction of 0.8982 and lower density regions of 0.67 m with an index of 0.9755. The index values correspond to a transmit radio frequency (RF) 3 MHz. The green line is the total reflectance plus transmittance and the blue line is the reflectance alone.

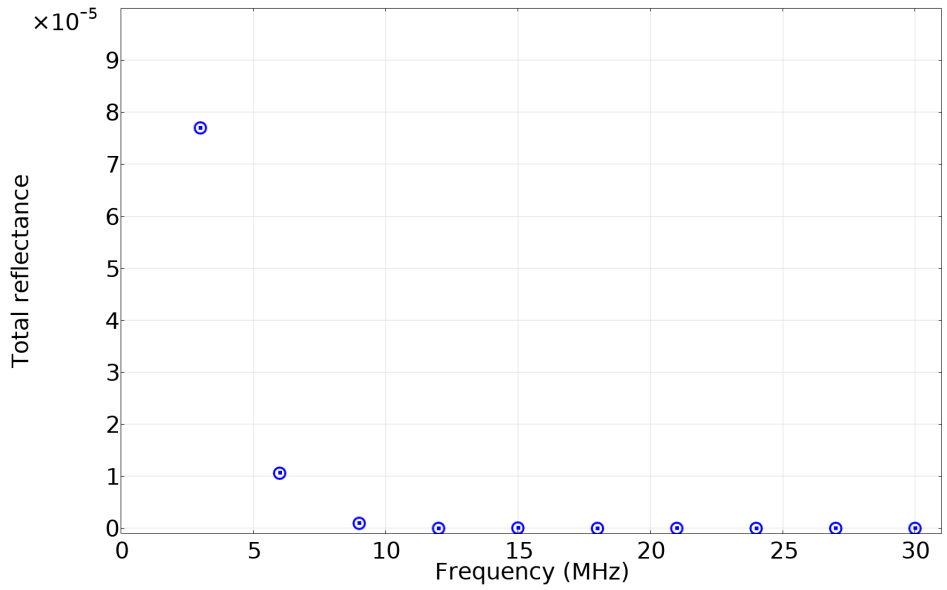

Fig. 7: RF frequency versus total reflectance. For each data point, the indices of refraction used are calculated for the corresponding frequency.

5. SOLITON SIGNATURE RETURN

An HF wave incident on a soliton scatters according to the plasma density and shape of the plasma soliton. The resulting scatter can be weakly refracted or strongly refracted, predominantly based on the density of the plasma. The path the resulting scatter takes through the ionosphere is not a linear trajectory and is strongly influenced by the ionosphere plasma density and gradient, and the Earth's magnetic field. The return path to the transmitter is a complicated one and is represented by challenge C in Fig. 1.

For a wave that is incident upon a soliton plasma density variation, there are two cases of interaction that should be considered:

1. The density change is significant enough to cause a reflection ($X = 1$)
2. The density change is too weak to cause a reflection ($X < 1$)

When a wave is incident on a soliton, the scatter appears to be according to the shape of the density perturbation and the absolute density. To understand the mechanics, we place a region with a plasma density change in the path of the ray in our ray tracer. A Gaussian perturbation sphere is characterized by a radial density profile that follows a Gaussian distribution, where the density smoothly decreases from the center and asymptotically approaches the background density at the sphere's boundary. This is defined by

$$Density = m \cdot N_e \cdot \exp(-dr^2/rs^2),$$

where m is the increase in density of the soliton peak as a scaling value, N_e is the Ionosphere background plasma density in that location, and dr^2 is the distance from the center of the perturbation, defined as $dx^2 + dy^2 + dz^2$. The variables dx, dy, and dz are the differences between the ray location and the perturbation location in ECEF coordinates. The variable r is the size of plasma disturbance used in this section to illustrate the effects of an HF wave traced through the plasma, and is set to be 1 m for the cases presented.

Fig. 8 shows rays being incident on different levels of plasma density perturbation. Each ray is incident normal to the plasma perturbation, which is in the shape of a sphere and has an exponential increase of density. The refraction of a ray occurs according to the magnitude of the density increase. The critical factor at 126.2 km in the absence of a perturbation is $X \approx 0.38$, which requires a plasma increase of greater than 2.63 times for direct reflection.

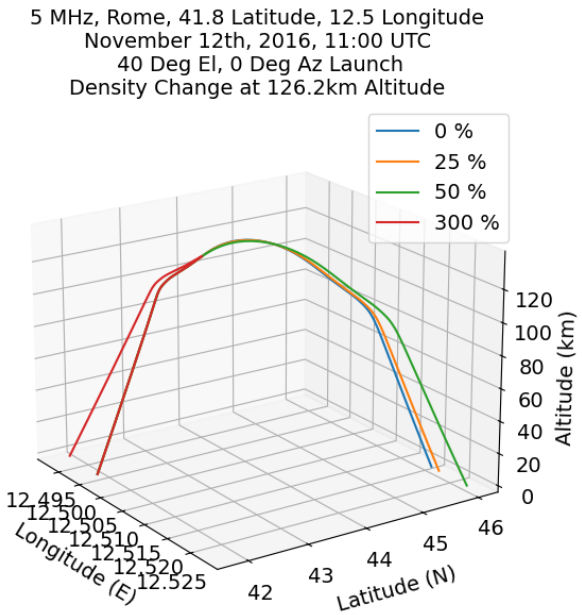

Fig. 8: Ray incident on spherical Gaussian density perturbation for various density changes.

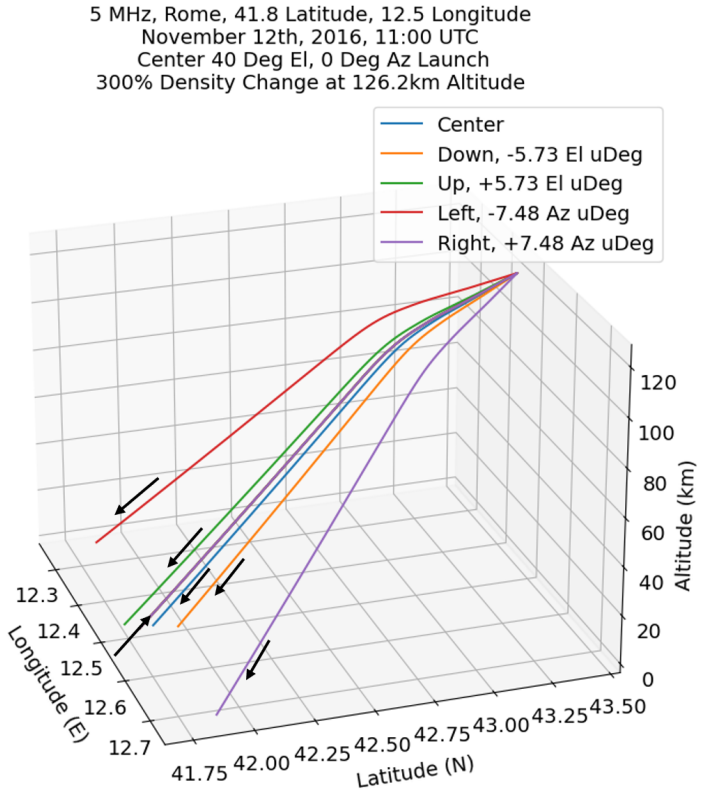

Fig. 9: A plane wave modeled as 5 points (center, down, up, left, right) is incident on a spherical plasma perturbation. Power incident upon a plasma perturbation will radiate back toward the transmitter according to the orientation of the wave incident on the plasma disturbance and the magnitude of the perturbation. This demonstrates that if the wave is reflected, some amount of the power will likely return to the transmitter.

While a single traced ray does not necessarily return to the transmitter, the power appears to reflect as if off a convex surface, as is seen in Fig. 9. This provides an indication that even though the path through the ionosphere is not linear, there is a reasonable indication power can make its way back to the transmitter.

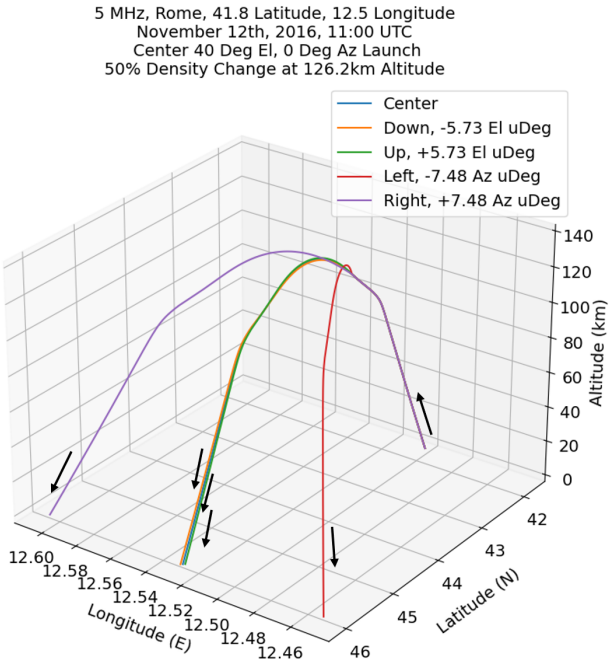

Fig. 10: Scattering pattern of an incident plane wave modeled as 5 points (center, down, up, left, right) interacting with a 50% plasma density perturbation. The density is not high enough to reflect the wave and instead lenses it. The center line is stacked on the up and down lines.

For the case where power does not reflect due to the critical factor being too low, the wave can still be refracted and deviate from the nominal trajectory. Fig. 10 shows the results of a plane wave, modeled as 5 points (center, down, up, left, right), interacting with a plasma density perturbation that has a critical factor of less than 1 for the given transmit frequency. The lensing results in the plane wave spreading out, indicating that nulls in the power received may be just as informative as increases in received power from an echo.

While it may be possible for power echoing off a soliton to be detectable, it can be seen in the ray tracing graphs that the path the ray takes is not a straight line. The group velocity of the wave can be significantly below the vacuum speed of light as the ray passes through the plasma, indicating that both the path taken and the speed along the path are not easily determined. Triangulation of a soliton echo is theoretically possible because power is reflected. However, sufficient receiver signal-to-noise ratio (SNR) and sophisticated triangulation techniques will be required.

For plasma disturbances where the critical factor is less than one as seen for Fig. 10, careful choices of launch angles and receiver locations will be key to measuring the effect of the soliton perturbation upon the transmitted signal and for performing localization.

While this analysis is performed for low altitude probing from the ground, research suggests solitons may not be formed at altitudes below 1000 km [14, 15]. Even so, the fundamental mechanics still hold true if the signal is emitted from a satellite and used to probe the ionosphere from space.

6. CONCLUSIONS

The detection of small (< 1 cm) LNTs is beyond the capabilities of our current detection systems and yet the need for the detection of these objects increases with their growing prevalence. Here we investigate the existing critical challenges of implementing a ground-based end-to-end soliton detection system for the identification and tracking of

LNTs. When approaching this problem with HF radiation, we highlight three challenges to realization of this system. These include (1) the HF radar signal must be above 10 MHz in order for the wave to propagate through the ionosphere to the debris and corresponding soliton of interest; (2) limiting the spectral range to above 10 MHz negates the ability of the soliton to reflect the incident wave for a set of realistic space soliton parameters and the corresponding plasma density changes; (3) the path distortion through the ionosphere results in a return signal that may or may not be at the transmitter location and the path traced is dependent on the soliton itself.

Our research demonstrates initial challenges for a fully ground-based system; further research is needed to overcome the above-described obstacles. Space-systems, either fully space-based or hybrid space-ground systems, remove the first obstacle of propagation through the ionosphere as this propagation is not needed for arrival to the LNT. Frequencies in the lower part of the HF spectrum, where the soliton return is stronger, could then be utilized for LNT detection via plasma solitons.

7. ACKNOWLEDGMENTS

We acknowledge the Community Coordinated Modeling Center (CCMC) at Goddard Space Flight Center for the use of the IRI 2016 and 2020 models in generating inputs to other software used in this paper. Models can be accessed at `https://ccmc.gsfc.nasa.gov/models/IRI~2016/` and `https://ccmc.gsfc.nasa.gov/models/IRI~2020/`.

This research is based upon work supported in part by the Office of the Director of National Intelligence (ODNI), Intelligence Advanced Research Projects Activity (IARPA), via 2023-23060200005. The views and conclusions contained herein are those of the authors and should not be interpreted as necessarily representing the official policies, either express or implied, of ODNI, IARPA, or the US Government. The U.S. Government is authorized to reproduce and distribute reprints for governmental purposes notwithstanding any copyright annotation therein.

8. REFERENCES

[1] Digital repository at the University of Maryland (DRUM). `https://drum.lib.umd.edu`. Accessed: 2024-08-30.

[2] P. A. Bernhardt, L. Scott, A. Howarth, and G. J. Morales. Observations of plasma waves generated by charged space objects. *Physics of Plasmas*, 30(9):092106, 2023.

[3] COMSOL. Comsol Multiphysics® v. 6.2, 2024.

[4] I. M. DesJardin and C. M. Hartzell. Nonlinear spectral analysis of ion acoustic solitons arising from a streaming charged object using the numerical inverse scattering transform. *Physics of Plasmas*, 29(11):112116, 11 2022.

[5] I. M. DesJardin and C. M. Hartzell. Ionospheric interaction based detection of sub-centimeter space debris. In *Proceedings of the Advanced Maui Optical and Space Surveillance Technologies Conference*, 2023.

[6] M. Fontell. Numerical ray tracing of medium and high frequency radio waves in the terrestrial ionosphere.

[7] The MathWorks Inc. Matlab version: 9.11.0 (r2021b), 2021.

[8] The MathWorks Inc. Signal processing toolbox version: 9.11 (r2021b), 2021.

[9] R. M. Jones and J. J. Stephenson. A versatile three-dimensional ray tracing computer program for radio waves in the ionosphere, October 1975.

[10] L. D. Landau and E. M. Lifshitz. *Electrodynamics of Continuous Media*, volume 8 of *Course of Theoretical Physics*. Pergamon Press, Oxford, 1960.

[11] M. Matney. Measuring small debris - what you can't see can hurt you.

[12] A. Sen, S. Tiwari, S. Mishra, and P. Kaw. Nonlinear wave excitations by orbiting charged space debris objects. *Advances in Space Research*, 56(3):429–435, 2015. Advances in Asteroid and Space Debris Science and Technology - Part 1.

[13] M. I. Skolnik. *Radar Handbook*. McGraw-Hill Education, New York, 3rd edition, 2008.

[14] A. S. Truitt and C. M. Hartzell. Characteristics of plasma solitons produced by small orbital debris. In *First Int'l. Orbital Debris Conf.*, 2019.

[15] A. S. Truitt and C. M. Hartzell. Simulating plasma solitons from orbital debris using the forced Korteweg-de Vries equation. *Journal of Spacecraft and Rockets*, 57(5):876–897, 2020.